

DATA-DRIVEN TLP TENDON LOADS FROM INTERNAL HULL FIBER-OPTIC SENSORS

John D. Hedengren^{1,*}, David Brower^{2,*}, Kody Kidder³, Zachary Hillman¹

¹Brigham Young University, Provo, UT

²Astro Technology, Houston, TX

³EnVen Corporation, Houston, TX

ABSTRACT

A new and innovative monitoring system is based on fiber-optic sensors and has been developed and installed on a Tension Leg Platform in the Gulf of Mexico. The system design is implemented to replace standard load cells that have been the workhorse of providing tendon load data over the last two decades. Many load cells have been efficient but have reached the end of life and on most Tension Leg Platforms have either failed or have degraded performance. The new monitoring system is based on a data-driven model to infer tendon load data from internal hull fiber-optic sensors. There are no subsea parts and all sensors, cabling, and hardware is located topside. This method involves several hundred Fiber Bragg Grating sensors that are placed on a webframe within the hull of the Tension Leg Platform. The location of the sensors is based on a detailed Finite Element Analysis and maximized correlation between webframe strain and tendon load. One year of fiber-optic sensors data (700 GB) trains regression models that correlate webframe strain to tendon loads. The new sensors and predictive models provide measurements within 0.8% mean absolute percentage error of the original load cells over the course of several months. This equates to +/- 40 kips (40,000 lbf) on each of the six tendons during wave action, tide fluctuations, storms, and strong loop currents. A resolution of 100 kips (100,000 lbf) is required for verification within a weight triangle, showing the feasibility of this system to replace the load cells. There are several new innovations and features with this new system that are reported here. The sensing system is dry-installed in the ballast tanks of the Tension Leg Platform with sensor orientation designed to maximize correlation between tendon load and fiber-optic sensor strain variation. All electronic components are topside with cabling penetrations into the ballast tanks. The fiber-optic sensors are multiplexed together to minimize cabling and maximize sensor count. These fiber-optic sensors immune to electromagnetic interference and corrosion. The data-driven model from the fiber

optic sensor data is integrated directly into the existing Integrated Marine Monitoring System. There is direct correlation of tendon loads with the new sensors when trained with the remaining load cell sensors. The fiber-optic sensors collect strain measurements at 1000 Hz and report new load measurements with 100 measurements consolidated into one load value sent every 0.1 seconds. There are consistent data measurements and reliable analysis of peak displacement from each of the sensors with resolution less than 0.1 nm. For comparison, the diameter of an iron atom is 0.126 nm. The data is divided into training and test sets with one year of training and a shorter period of validation. The training and validation include assessment of environmental effects such as wave action, tide cycles, storms and excessive weather, and annual water temperature changes in the Gulf of Mexico. Fiber-optic temperature gauges are installed on the webframes and compensation is built into the regression algorithm.

Keywords: Tension Leg Platform, Load Monitor, Internal Hull, Fiber Optic, Strain

NOMENCLATURE

Acronyms

FBG	Fiber Bragg Grating
GOM	Gulf of Mexico
IH	Internal Hull
IH1	Internal Hull, Sensor Set 1
IH2	Internal Hull, Sensor Set 2
IMMS	Integrated Marine Monitoring System
LC	Load Cell
MAPE	Mean Absolute Percentage Error
OLS	Ordinary Least Squares
ROV	Remotely Operated Vehicle
TLP	Tension Leg Platform

1. INTRODUCTION

A fiber-optic sensor-based monitoring system has been developed and installed on the Neptune Tension Leg Platform (TLP)

*Corresponding author: dbrower@astrotechnology.com

in the Gulf of Mexico (GOM). The Neptune TLP began production in 2008 and is located 120 miles offshore Louisiana in water depths ranging from 4,200 to 6,500 feet. It is equipped to handle up to 50,000 barrels of oil and 50 million cubic feet of natural gas per day through six subsea wells. The fiber optic system was implemented to replace the standard load cells that have been used to provide tendon load data on TLPs for the past 15 years, many of which have either failed or experienced decreased performance due to age.

1.1 Load Cells for Tendon Tension Monitoring

Load cells are devices that are used to measure force or weight. They are often used in industrial and scientific applications to accurately measure the tension or compression forces applied to an object. In the case of a TLP, load cells are used to monitor the tension in the tendons that support the platform.

TLPs are floating platforms used in offshore wind energy and oil and gas production. They are anchored to the seafloor by long tendons, which are typically made of steel cable. The tendons are subjected to tension forces due to the weight of the platform and the buoyancy forces acting on it. Load cells are used to measure the tension in the tendons, which helps to ensure that the platform is stable and that the tendons are not subjected to excessive forces that could cause them to fail. Fig. 1 shows the Neptune TLP shifted off-center due to wind and current forces. The base-line tendon tensions are in the range of 3600–3900 kips (16,014–17,348 kN). Wave action amplitude is typically 10–80 kips (44–356 kN) with a period of 4–7 sec, but the amplitude can exceed 200 kips (890 kN) during storms. Tide action tendon tension amplitude is typically 40–80 kips (178–356 kN). One of the notable features of the GOM is its loop current that flows through the Gulf. The loop current is formed by the warm, saline water that flows northward from the Caribbean Sea and the Yucatan Channel, and is then deflected eastward by the Gulf Stream. Sometimes the strong loop currents in the GOM reach the Neptune TLP and put additional tension on the tendons. The tendon tensions shift due to topside load changes, loop current, platform tilt, wave, and wind forces. Re-ballast operations typically occur only during inspection operations in the pontoons to remove ballast water from tip tanks or with significant heavy lift operations to compensate for new topside equipment. The ballast operations are designed to keep the platform within a weight triangle that provides guidance on a safe operating window for deviations of center of gravity and tendon tensions.

The load cells on many TLPs fail. One common cause of failure is water ingress and corrosion, which can occur when the load cells are exposed to harsh environments such as sea water. Load cells also fail due to mechanical wear and tear or due to electrical issues such as voltage spikes on a particular bridge. In some cases, load cells may also fail due to manufacturing defects or improper maintenance. Load cells are designed at the top of the tendon where it attaches to the platform. The load cells are typically submerged where cathodic protection and robust seals are required to maintain the electrical and mechanical components. Repairing or replacing the load cells is often not economically feasible due to the subsea location and challenges with unloading the tendon tension for replacement and calibration.

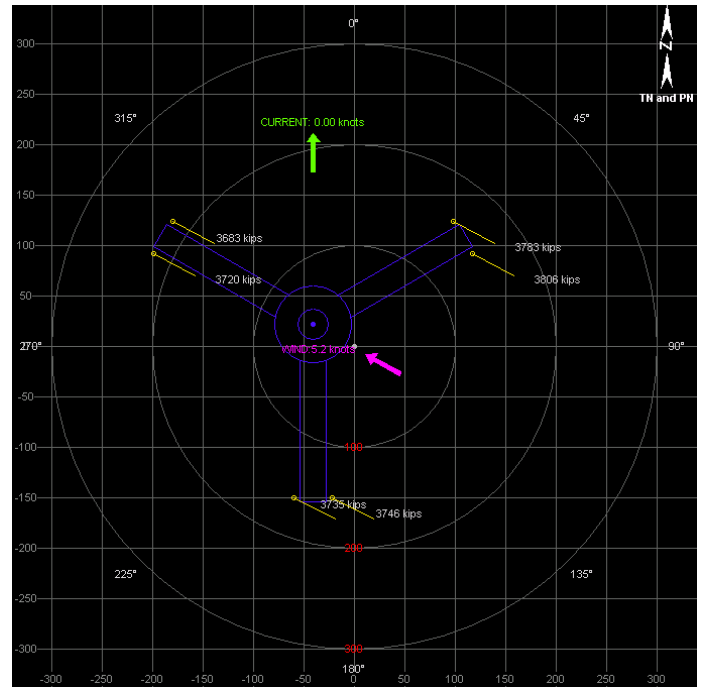


FIGURE 1: PLATFORM POSITION AND TENDON TENSIONS SHIFT WITH WIND, WAVES, AND WATER CURRENTS.

Out of the 36 original load cells, only 11 are still functioning properly. It is challenging to repair or replace the faulty load cells. Without a backup system and with more load cells failing, the platform could lose the ability to monitor tendon load. This is important for regaining access to the platform after a storm and for sea-worthiness certification. Therefore, it was necessary to find a new system that can be retrofitted and calibrated onto the existing platform in order to extend its service life without the need to replace the load cells themselves.

1.2 Tension Leg Platforms

TLPs are floating oil production platforms that are used for drilling and production operations in deepwater environments, such as the GOM. TLPs are designed to be stable and resistant to the forces of wind, waves, and currents, and are well-suited for use in deepwater environments where these forces can be significant [1]. TLPs consist of a floating platform supported by a series of tendons, which are long, flexible cables anchored to the sea floor. The tendons are kept under tension, which helps to keep the platform stable and upright. TLPs are typically designed with a triangular or square base, which provides a large area for drilling and production operations. TLP tendons and risers have been modeled with Finite Element Analysis (FEA) to design and optimize the operation [1–4].

1.3 Fiber-Optic Monitoring

Fiber-optic monitoring using fiber Bragg gratings (FBGs) is a technique for measuring strain and temperature using a fiber-optic sensor [5]. FBGs are small reflective structures that are inscribed directly into the core of a single-mode optical fiber. They are typically made by exposing the fiber to a periodic pattern of intense UV light, which creates a series of microscopic

refractive index changes in the fiber core. When light is transmitted through an FBG, the reflected spectrum of light has a narrow peak at a specific wavelength, known as the Bragg wavelength. This wavelength is determined by the periodic refractive index changes in the fiber, and is sensitive to changes in the strain and temperature of the fiber. To measure strain and temperature using FBGs, a light source is used to illuminate one end of the fiber, and the reflected spectrum of light is measured at the other end using an optical sensing module. By analyzing the position of the reflected spectrum, it is possible to calculate the strain and temperature of the fiber with high accuracy [6, 7].

FBGs are used to monitor TLPs because they are highly sensitive and can be easily attached to the tendons or hull of the TLP. In a TLP, FBGs can be used to measure the strain and temperature of the tendons [5, 8], which are under high tension and are subjected to significant forces and loads. By monitoring the strain and temperature of the tendons, it is possible to detect any changes or deformations in the tendons, which can be used to predict the structural integrity of the tendons of a TLP.

1.4 Point and Distributed Sensing

Fiber-optic point sensing with FBGs and distributed sensing with Brillouin scattering are both techniques for measuring strain, temperature, and other parameters using fiber-optic sensors. However, they differ in the way they measure these parameters and the types of applications they are most suited for.

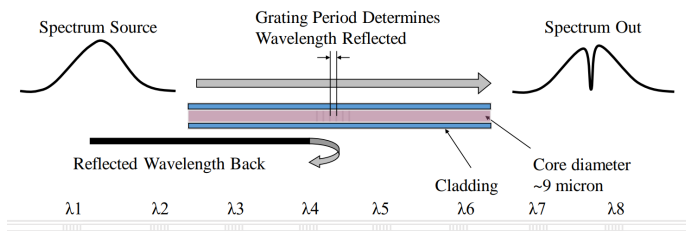


FIGURE 2: FIBER BRAGG GRATINGS (FBG) ETCHED INTO THE FIBER IN SERIES.

FBGs are small reflective structures inscribed directly into the core of a single-mode optical fiber as shown in Fig. 2. They work by reflecting a narrow peak of light at a specific wavelength which is determined by the periodic refractive index changes in the fiber. When the strain or temperature of the fiber changes, the Bragg wavelength shifts, allowing the FBG to measure these parameters with high accuracy. FBGs are typically used for point sensing, where a single or a few FBGs are used to measure the strain or temperature at a specific location on a structure or pipeline. The scan frequency is much higher than distributed sensing and 10 Hz to 5000 Hz sample frequency is typical with swept lasers in the 1480-1620 nm laser range as shown in Fig. 3. The natural attenuation of the light signal in this range is 0.285 dB/mi. The light travels to the sensor and back to the fiber-optic interrogator, making a round-trip journey that covers twice the distance of the fiber cable. This double distance is important in calculating the attenuation of the light signal and the shift that occurs with distance as the reflected light signal is analyzed. Increased distance also limits the scan frequency

as light time of flight becomes a limiting factor for the receiver to collect the return light before starting the next signal pulse. To improve the strength of the signal, a high-viscosity pressure-balancing fluid is applied over the fiber-optic strands to provide encapsulation. This is necessary for optimal performance in subsea conditions where pressure can cause deformation of the glass fibers or micro-bending when in contact with the structure surface. The high-viscosity fluid and armored sheathing is also used to prevent direct contact with the surfaces, which may have irregularities that could damage the fiber or cause high stress points.

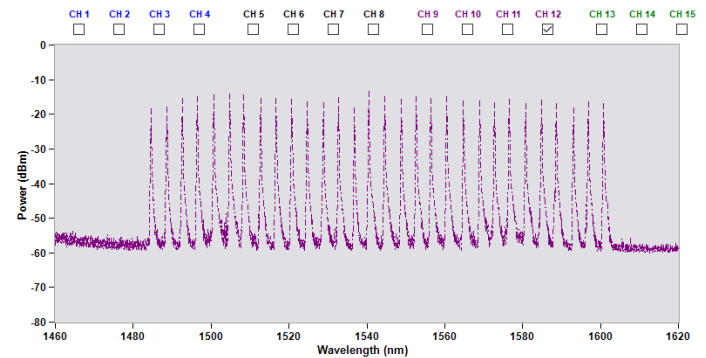


FIGURE 3: PEAK SIGNALS IDENTIFIED BY THE FIBER-OPTIC INTERROGATOR.

In addition to point sensing from FBGs, there are a multitude of distributive sensing methods that are sometimes used such as Brillouin, Raman, and Rayleigh. These fiber-optic methods rely on backscattered light. Distributed sensing with Brillouin scattering uses the scattering of light caused by thermal or density fluctuations in the fiber to measure strain and temperature over the distance of the fiber. In this technique, a laser is used to transmit light through the fiber, and the scattered light is detected from back-scatter or at the other end using a receiver. By analyzing the frequency shift of the scattered light, it is possible to calculate the strain and temperature along the length of the fiber. Distributed sensing with Brillouin scattering is suitable for measuring strain and temperature at intervals along the fiber and is often used to monitor pipelines and other large structures [9, 10]. There is a trade-off between the resolution of the measurements (e.g. every 1m versus 20m) and scan frequency (e.g. 1 min versus 10 sec).

FBGs are used for point sensing and can measure strain and temperature with high accuracy at a specific location, while distributed sensing with Brillouin scattering is used for long-distance sensing and can measure strain and temperature along the length of a fiber-optic cable.

1.5 Fiber-Optic Monitoring Solutions

Fiber-optic monitoring has a wide range of applications in the oil and gas industry, including for the monitoring of drilling risers, steel catenary risers, TLPs, touchdown zones, slugging mitigation, subsea tiebacks, and umbilical installations [11–16]. There have been recent developments in post-installable sensor stations that can be attached with adhesive for use in shallow waters [17], as well as friction-based solutions for deepwater Remotely Operated Vehicle (ROV) installation [18]. In addition,

this technology has been extended to distributed monitoring [19], with applications in leak detection [20] and the monitoring of cryogenic liquified natural gas transfer pipelines [21].

2. NEW DEVELOPMENTS: INTERNAL HULL FIBER-OPTIC MONITORING

The goal of this study is to explore a new application of FBG sensors, specifically by retrofitting sensors on webframes of the Internal Hull (IH) of pontoons on the Neptune TLP as shown in Fig. ??.

The alternative was to retrofit the platform with sensors that are placed directly on the tendons themselves with sat divers. Sat divers, or saturation divers, are divers who live and work in a pressurized environment for extended periods of time. Saturation diving is often used in offshore oil platform work because it allows divers to work at greater depths for longer periods of time without the need to surface and decompress. However, saturation diving comes with significant risks and dangers, including the risk of decompression sickness. Working on the interior of the hull of an oil platform is generally considered safer than working in the open water because it reduces the risk of exposure to harsh weather conditions and sea life, and it also allows for easier access to tools and materials. Additionally, working on the interior of the hull reduces the risk of diving accidents, such as those caused by entanglement in underwater debris or equipment.

2.1 Bulkhead Penetration

Certification of bulkhead integrity is a requirement for crossing bulkheads with fiber-optic cable routing and placing sensors in the pontoons. Watertight integrity is essential to reduce risks of single point of failure in floating structures. Bulkheads on the Neptune platform separate the tip tank, interior pontoon region, and the center cylindrical column. The sensor locations are on the K webframe in the pontoon interior region and R webframe in the ballast water tip tank (see Fig. 5).

The fiber-optic cables are routed through two MCT Brattberg cable penetrations per pontoon. During hydrostatic loading, an unexpected small leak was observed through the interior of the fiber-optic cable identified in Fig. 6a. The ballast water was transferred out of the tip tank for mitigation of the leak with a splice breakout connection to remove the pathway through the interior of the cable as shown in Fig. 6b. All bulkhead penetrations were certified and the ballast water in the tip tank returned to normal operating levels.

2.2 Finite Element Analysis for Gauge Placement

Finite Element Analysis (FEA) was used to simulate the loading conditions on the webframe and predict the strain distribution across the structure. FEA is used to analyze and predict the behavior of structures under different loading conditions such as wave action and tide cycles. It was used to determine the placement and orientation of fiber-optic strain gauges on the webframes (see Fig. 7).

To perform FEA for this purpose, a digital model of the webframe was created and divided into a series of smaller elements, each with a set of properties. The loading conditions on the webframe, such as the tendon tensions, were applied to the

model, and the resulting strain distribution calculated. By comparing the strain distribution sensitivity of the strain gauges, the locations and orientations of the gauges were determined to provide the highest sensitivity to the tendon tension changes. This approach allowed engineers to optimize the placement and orientation of the strain gauges without the need for physical testing, which is costly and time-consuming. It also allowed for more precise and accurate predictions of the strain distribution and the sensitivity of the gauges, which improved the accuracy of the load monitoring system.

2.3 Data Collection and Preprocessing

In this study, the process of preprocessing the data collected by the sensors was crucial. The sensors generated a large amount of data, approximately 2 GB per day, including FBG peak values from every sensor and readings from each load cell. The FBG sensors provided data at 1000 Hz and every 100 samples were averaged to provide peak values at a rate of 10 Hz. The tendon loads are calculated from the peak values and sent to the Integrated Marine Monitoring System (IMMS) through a Modbus connection. The number of FBG sensors by pontoon location and webframe is shown in Table 1. The sensors are located on two loops with Internal Hull 1 (IH1) and Internal Hull 2 (IH2). IH1 was installed one year earlier than IH2 as a proof-of-concept test of the monitoring system to verify that the locations and installation procedure are effective. Several modifications to the installation include surface preparation to passivate existing corrosion, relative humidity control during installation, and additional ruggedization of the cable in the tip tank.

TABLE 1: LOCATION AND NUMBER OF FBG SENSORS

Location	Webframe	IH1 Sensors	IH2 Sensors
Pontoon 1	K (Dry)	12	64
Pontoon 1	R (Wet)	14	30
Pontoon 2	K (Dry)	12	64
Pontoon 2	R (Wet)	14	30
Pontoon 3	K (Dry)	12	36
Pontoon 3	R (Wet)	14	30

This data is sent to a server by the fiber-optic interrogator and load management system. The data transfer is managed by multiple Modbus connections and the data is synchronized by the timestamps. However, there are sometimes interruptions in the data stream due to technical issues, maintenance, power outages, or platform shut-in during storms that resulted in gaps in the data. Additionally, as the load cells approached the end-of-life, readings drifted from those of the redundant counterparts. These and other data cleansing issues had to be addressed before an empirical model could be trained that relates webframe strain to tendon load.

3. SENSOR AND MODEL CALIBRATION

These sensors provide real-time measurements of the tendon tensions of the TLP. The section provides details on the correlation of the FBG sensor readings to the tendon tensions from load cell data. If load cell data did not exist, FEA simulated values

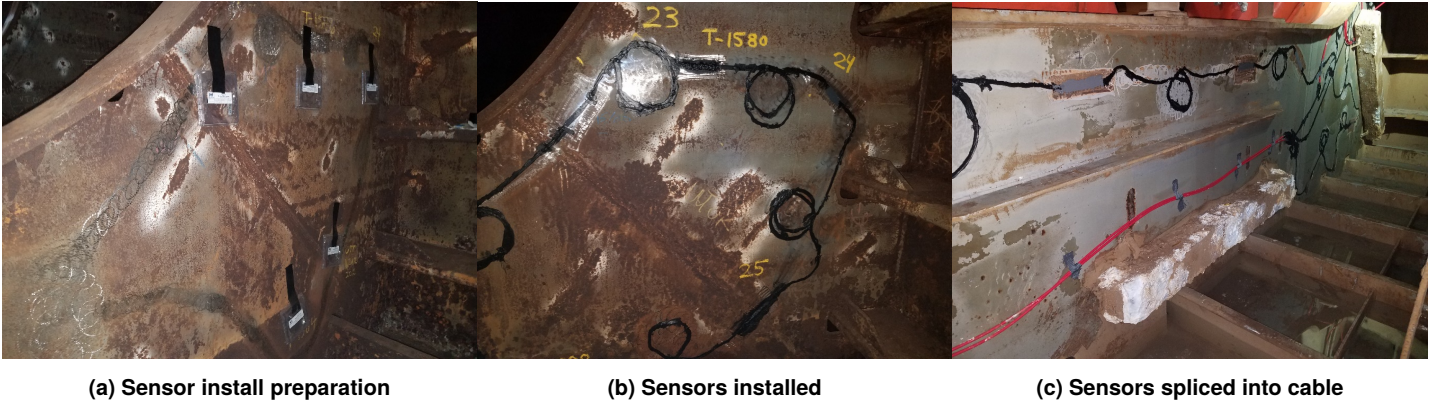


FIGURE 4: SENSOR LOCATION PREPARATION AND INSTALLATION.

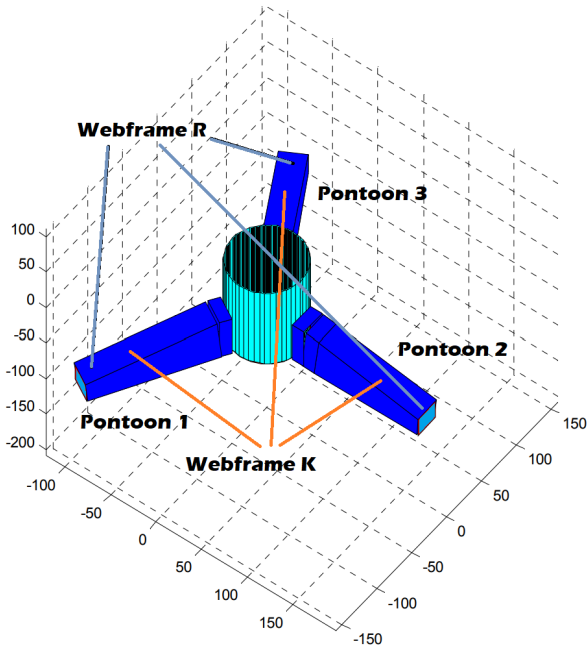


FIGURE 5: WEBFRAME LOCATIONS IN THE INTERIOR HULL FOR SENSOR INSTALLATION.

would be used for the calibration. The results and performance of the system over a year-long period are also reported.

Redundant sensors were installed to ensure that the required information could still be collected even if one of the sensors failed. In the case of IH2 sensors, two sensors were installed parallel to each other and two were installed perpendicular to the first two. These redundant signals are scored using a Feature score (F score) to determine the importance of each as shown in Fig. 8 for Pontoon 1. The feature score calculates the average reduction in accuracy due to leaving out a particular sensor. A larger decrease in accuracy corresponds to a more important feature. The sensor identification has a number (pontoon), letter (K or R webframe), sensor location (number) and orientation (A-D).

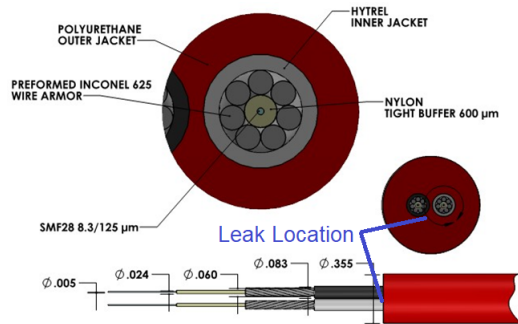
The most important sensors are on webframe K. The least important sensors for predicting load are the temperature compensation sensors. This is expected because they are detached from the strain field and only measure temperature fluctuations. Additional logic is implemented to determine the best use of the redundant signals. If one of the redundant sensors scored slightly higher than the sensor counterpart, the counterpart sensor was dropped and vice versa. If there are fewer independent sensors available than sensors required, the complimentary are used regardless of the redundancy.

The models in this study are trained using data from July 2021 to July 2022 and tested on data from October 2022. The testing period was chosen because it includes a full annual cycle of temperature changes as shown in Fig. 9.

A ballast shift occurred in July 2021 and January 2022. The training also includes GOM storms that caused the full range of expected TLP tensions. The training data is shuffled randomly to remove any time-series features. The mean absolute percentage error (MAPE) is the basis for the evaluation. A target accuracy is 1% MAPE or about 40 kips.

Linear regression correlates FBG sensor peak wavelengths to Load Cell (LC) tendon tensions. Linear regression is a simple model that is used to predict a continuous response variable based on one or more predictor variables. It assumes that the relationship between the predictor and response variables is linear as shown with Eq. 1.

$$\ell = P\beta + \epsilon \quad (1)$$



(a) Cable sheathing leak location



(b) Solution to seal fiber-optic cable

FIGURE 6: IDENTIFICATION AND MITIGATION OF BALLAST WATER PATHWAY THROUGH THE FIBER-OPTIC CABLE SHEATHING.

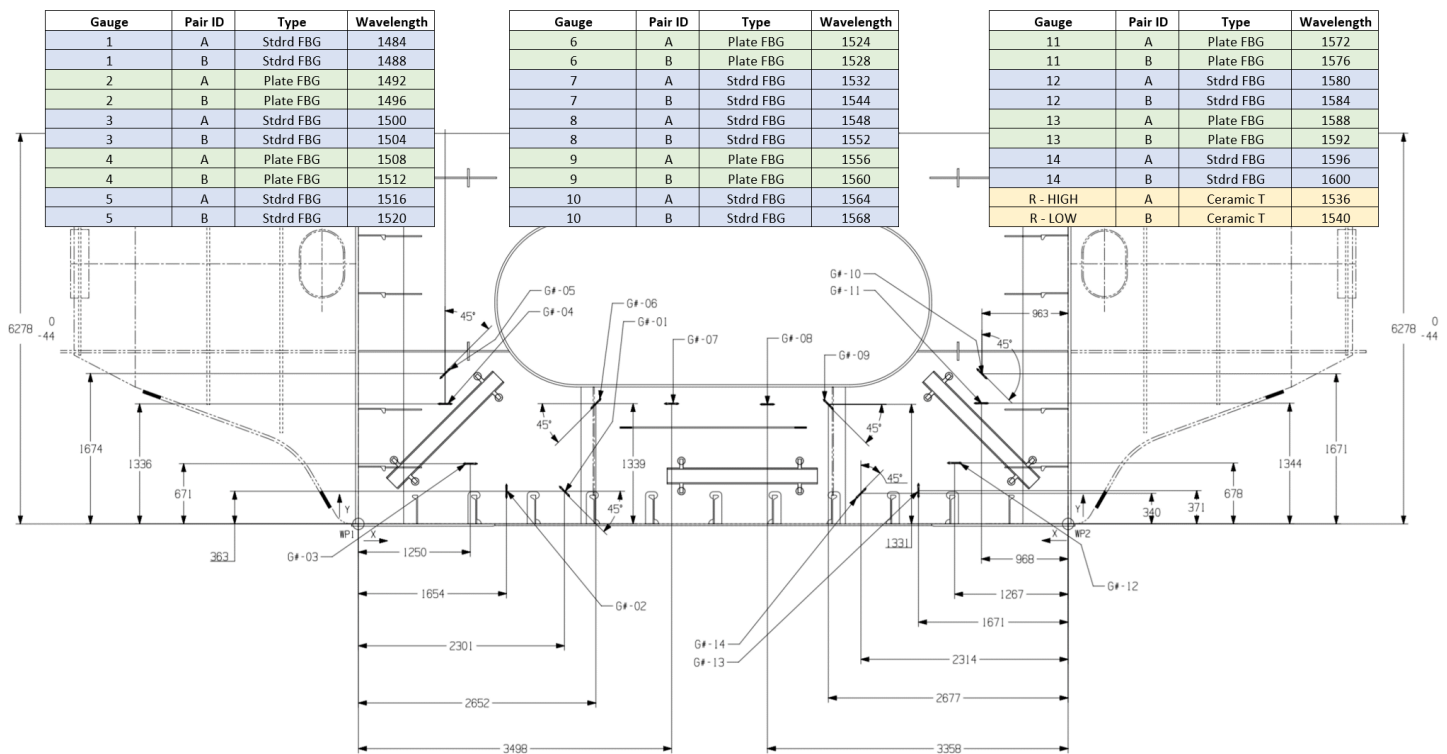


FIGURE 7: FBG GAUGE LOCATIONS ON WEBFRAME R SELECTED BY FEA ANALYSIS.

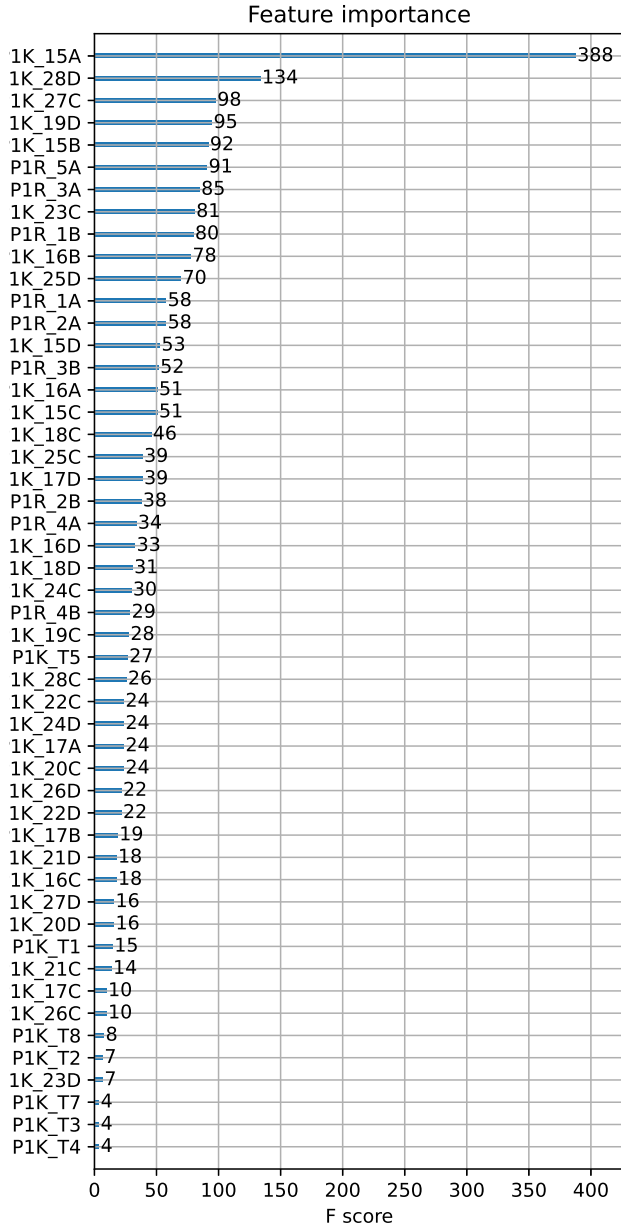


FIGURE 8: F IMPORTANCE RANKING OF SENSORS.

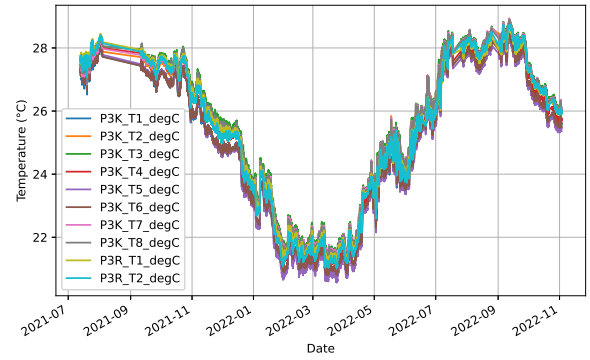


FIGURE 9: TRACKING SEASONAL CHANGES IN PONTON 3 FOR TEMPERATURE COMPENSATION.

where ℓ is the load, P is a vector of peak wavelengths, β is a vector of regressed parameters, and ϵ is the measurement error. The parameters β are obtained by minimizing the difference between the predicted and measured loads as shown in Eq. 2 with the Python statsmodels function for Ordinary Least Squares (OLS).

$$\min_{\beta} \left(\sum_{i=1}^n \epsilon_i^2 \right) \quad (2)$$

Linear regression is easy to interpret and is computationally efficient, but it is limited to modeling linear relationships and do not perform well on more complex datasets. A variety of more complex models are evaluated including Multilayer Perceptrons (Artificial Neural Network), Boosted Gradients (XGBoost regression), k-Nearest Neighbors, and Support Vector Regressor (SVR) in a forthcoming journal publication. Linear regression is superior on the validation dataset because of the extrapolation potential, ability to train on more data, and the linear relationship between wavelength peak and tendon tension. Scale-up to larger data sets is computationally linear with a variety of software packages as shown in Fig. 10.

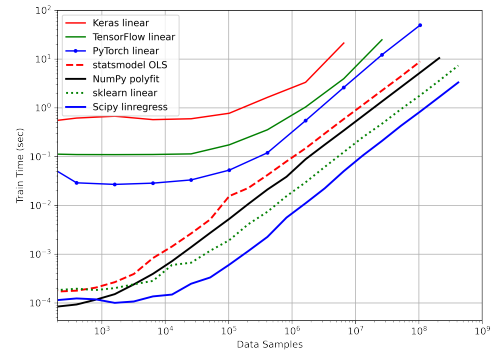


FIGURE 10: COMPUTATIONAL SCALE-UP OF LINEAR REGRESSION WITH PYTHON PACKAGES.

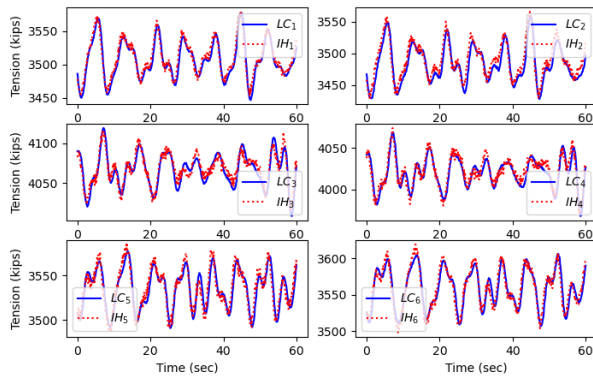


FIGURE 11: COMPARISON OF LOAD CELL (LC) AND INTERNAL HULL (IH) FIBER-OPTIC MEASUREMENT OF TENDON TENSION.

This computational scale-up is important for the IH regression because of the potential large number of data points. Data is recorded over 12 months at a rate of 10 Hz for a total of 3.1×10^8 data points. Similar regression results are obtained when downsampling by 100x, so this quantity of data is not needed in practice.

3.1 Model Performance

IH fiber-optic gauge performance is evaluated on two principal qualifications: (1) agreement with load cell measurement in magnitude of peak-to-trough range and (2) long-term mean load agreement to guide ballast operations for weight triangle determination. The first evaluation is shown in Fig. 11 with typical wave action over a 60 sec window. There is agreement between the load cell (LC) and IH measurements. The LC measurements are reported at 12 Hz while the IH measurements are reported at 10 Hz.

One observation during the evaluation of the fiber-optic monitoring system is that ballast water sloshing in the tip tank leads to perpendicular forces on the webframe, causing temporary shifts in the apparent load measurements. This is illustrated in Fig. 12, which shows the impact of IH ballast waves on the webframe. These shifts are undesirable because they can introduce error and uncertainty into the load measurements, potentially affecting the accuracy and reliability of the system. Load cell data was used for training, but the load cells can fail or degrade in performance over time, leading to mismatches in the measurement data. As shown in Fig. 12, the mismatch on LC₂ is due to a failure of the remaining load cells for tendon 2. To address this issue, the fiber-optic monitoring system provides replacement measurements for tendons where the load cells have failed. By using IH sensors and data-driven models, the system infers tendon load data with a high degree of accuracy, even when some of the load cells are no longer functioning.

The second evaluation of the fiber-optic monitoring system focuses on the long-term bias of the sensors and the ability to withstand seasonal temperature variations and maintain a long service life. To assess these aspects of the system, calibration and validation data was collected and analyzed, as illustrated

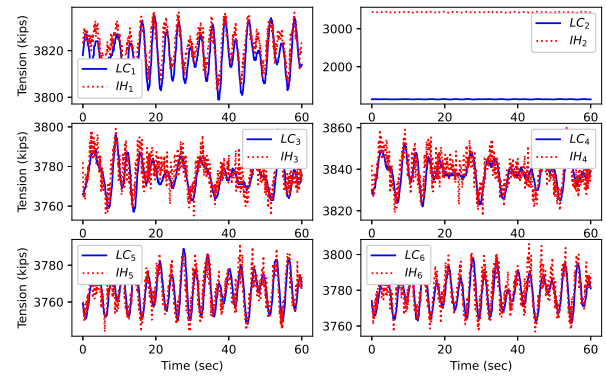


FIGURE 12: COMPARISON OF LOAD CELL (LC) AND INTERNAL HULL (IH) FIBER-OPTIC MEASUREMENT OF TENDON TENSION.

in Fig. 13. The long-term bias of the sensors refers to the ability to accurately measure tendon tensions over an extended period of time, without significant drift or deviation from true values. This is important because it ensures the reliability and consistency of the system's measurements, even under different environmental conditions. To withstand seasonal storms, the sensors were designed with a ruggedized construction that is resistant to temperature changes and other environmental stresses. This helps to extend service life and maintain accuracy over time. By analyzing the training data, it is possible to evaluate the long-term bias and ruggedized design of the sensors and determine suitability for long-term use in the fiber-optic monitoring system. These results are used to further refine and optimize the system to ensure reliable and accurate performance over the long term.

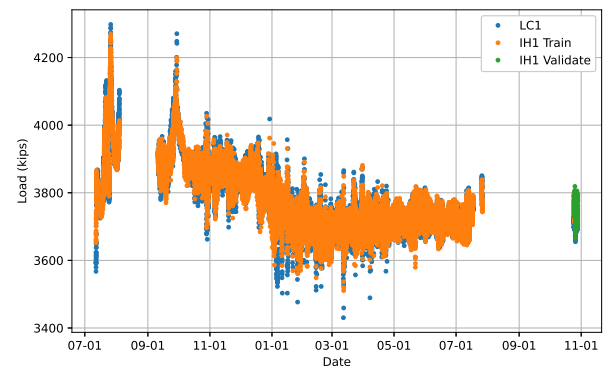


FIGURE 13: TRAINING FROM JULY 2021 TO JULY 2022.

The predictive linear models developed for the fiber-optic monitoring system have been shown to provide highly accurate tendon tensions, with a MAPE of 0.8% compared to the load cells over the training and validation periods. This level of accuracy is essential for the reliable and effective operation of the system and the safety of the offshore platform. The validation period for the models began at a specific point in time, which is illustrated in Fig. 14. During this period, the tendon tensions were affected

by daily sinusoidal changes due to tide cycles, as well as scatter caused by wave action with a period of 4-7 seconds. To further verify the accuracy and reliability of the models, additional validation is currently underway with third-party verification of the results. These results will be reported in a follow-on publication once they have been thoroughly assessed. Overall, the predictive linear models developed for the fiber-optic monitoring system have demonstrated an ability to provide accurate and reliable tendon tension measurements, which is critical for the safe and effective operation of the platform.

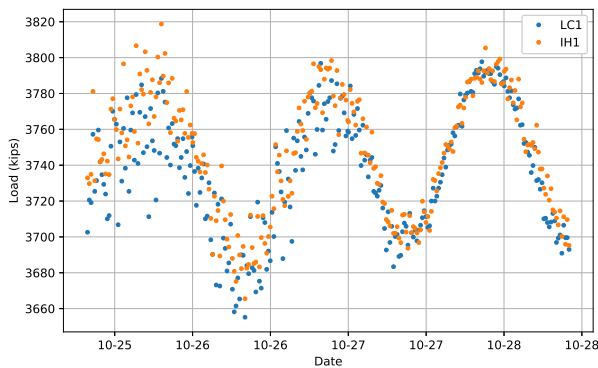


FIGURE 14: VALIDATION IN OCT 2022 WITH DAILY TIDE CYCLES AND WAVE ACTION.

Sufficient tendon tension accuracy is obtained from the K-only webframe sensors in the dry bulkhead for tendon tension measurements. The model is calibrated using the K-only webframe and K/R webframe sensors for comparison as shown by the regression parameters in Fig. 15. Tip tank sensors on the R webframe are not used in the final regression to avoid issues with ballast water sloshing that causes instantaneous shifts in the predicted tendon tensions.

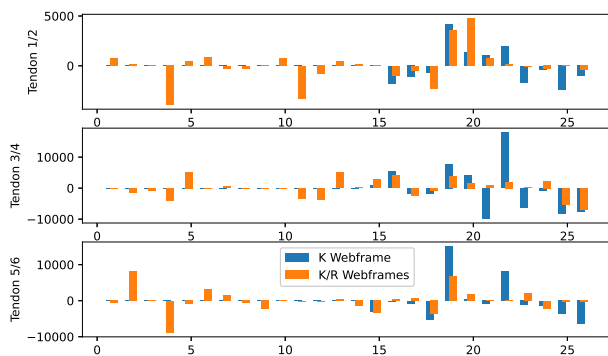


FIGURE 15: CONTRIBUTIONS OF EACH SENSOR LOCATION IN THE R WEBFRAME (1-14) AND K WEBFRAME (15-26).

The elimination of webframe sensors in the tip tank (R) of the platform improves the long-service life potential of the monitoring system for several reasons. First, the predictions made

by the system are not subjected to the wave action and potential cable damage that can occur in the ballast water of the tip tank. This can help to reduce wear and tear on the sensors and extend their lifespan. Additionally, by locating all sensors for tendon predictions in the dry bulkhead area of the pontoon, there is less potential for mechanical effects on the sensors from platform ballast water movement and ballast transfers. These movements cause stress and strain on the fiber-optic cables, which can lead to failure over time. By locating the sensors in a more stable and protected environment, the risk of mechanical damage is reduced, further improving the long-service life potential of the monitoring system.

Future work is needed to explore higher frequency data to 5000 Hz to evaluate the detection of Vortex induced vibration (VIV). VIV can cause the tendon to oscillate or vibrate, which can have negative consequences on the structural integrity. VIV on tendon tension can lead to increased fatigue on the tendons, which can ultimately reduce lifespan and lead to failure. It is important to monitor and mitigate VIV to ensure the safety and stability of offshore platforms. One way to do this is by using a monitoring system, such as the fiber-optic sensor system, to continuously measure and track tendon tension and track service life of the tendons.

4. CONCLUSION

In conclusion, a new fiber-optic sensor-based monitoring system has been developed and installed on a TLP in the GOM as a replacement for standard load cells. The predicted load values are trained with one year of data and validated two months after the training period. The validation includes baseline tendon tension as well as wave and tide cycle assessment. The system utilizes a data-driven linear regression model and internal hull fiber-optic sensors to infer tendon load with a mean absolute percentage error of 0.8%. The system has several innovative features, including dry-install in the ballast tanks, multiplexed sensors to minimize cabling, and integration with the existing IMMS.

ACKNOWLEDGMENTS

We acknowledge BHP and EnVen Corporation for support in project management and the WolfStar team for assistance with True-load software analysis for strain gauge placement. Fiber-optic technicians from NKT Photonics provided invaluable expertise and contributions to the project and BMT assisted with communication to the IMMS.

REFERENCES

- [1] Low, Y.M. "Frequency domain analysis of a tension leg platform with statistical linearization of the tendon restoring forces." *Marine Structures* Vol. 22 No. 3 (2009): pp. 480–503. ID: 271453.
- [2] Rustad, Anne M., Larsen, Carl M. and Sørensen, Asgeir J. "FEM modelling and automatic control for collision prevention of top tensioned risers." *Marine Structures* Vol. 21 No. 1 (2008): pp. 80–112. URL <https://www.sciencedirect.com/erl.lib.byu.edu/science/article/pii/S0951833907000263>. ID: 271453.

- [3] Janwar, Muhammad, Juswan and Alie, Muhammad Zubair Muis. "Tendon analysis on tension leg platform." *IOP Conference Series.Earth and Environmental Science* Vol. 575 No. 1 (2020). Source type: Scholarly Journals; Object type: Article; Object type: Feature; Copyright: © 2020. This work is published under <http://creativecommons.org/licenses/by/3.0/> (the "License"). Notwithstanding the ProQuest Terms and Conditions, you may use this content in accordance with the terms of the License.; DOI: 10.1088/1755-1315/575/1/012198; MSTARLegacyID: NWJPPFRN20201001v575n1E5751198.
- [4] Du, Zunfeng, Li, Xiaochen, Xu, Wanhai, Zhu, Haiming, Feng, Jiaguo, Shen, Wenjun and Jin, Ruijia. "An experimental investigation on vortex-induced motion (VIM) of a tension leg platform in irregular waves combined with a uniform flow." *Applied Ocean Research* Vol. 123 (2022): p. 103185. URL <https://www.sciencedirect.com/erl.lib.byu.edu/science/article/pii/S0141118722001286>. ID: 271423.
- [5] Dhingra, Ishant, Kaur, Gurpreet and Kaler, R. S. "Design and analysis of fiber Bragg grating sensor to monitor strain and temperature for structural health monitoring." *Optical and Quantum Electronics* Vol. 53 No. 11 (2021): p. 619. URL <https://doi.org/10.1007/s11082-021-03270-7>. ID: Dhingra2021 Summary: Bragg grating sensors are described and its behavioral model is given.
- [6] Sahota, Jasjot K., Gupta, Neena and Dhawan, Divya. "Fiber Bragg grating sensors for monitoring of physical parameters: a comprehensive review." *Optical Engineering* Vol. 59 No. 6 (2020): pp. 1–35. URL <https://doi.org/10.1117/1.OE.59.6.060901>.
- [7] Mieloszyk, Magdalena and Ostachowicz, Wiesław. "An application of Structural Health Monitoring system based on FBG sensors to offshore wind turbine support structure model." *Marine Structures* Vol. 51 (2017): pp. 65–86. URL <https://www.sciencedirect.com/science/article/pii/S0951833916302441>. ID: 271453 This article is a very similar case study to ours.
- [8] Mieloszyk, Magdalena, Majewska, Katarzyna and Ostachowicz, Wiesław. "Application of embedded fibre Bragg grating sensors for structural health monitoring of complex composite structures for marine applications." *Marine Structures* Vol. 76 (2021): p. 102903. URL <https://www.sciencedirect.com/science/article/pii/S0951833920301921>. ID: 271453 This paper focuses on the embedding of FBG sensors in a ship's hull to detect deformations.
- [9] Schenato, Luca. "A review of distributed fibre optic sensors for geo-hydrological applications." *Applied Sciences* Vol. 7 No. 9 (2017): p. 896.
- [10] Bao, Xiaoyi and Chen, Liang. "Recent progress in distributed fiber optic sensors." *sensors* Vol. 12 No. 7 (2012): pp. 8601–8639.
- [11] Brower, David V and Prescott, Neal. "Real time subsea monitoring and control smart field solutions." *Subsea Rio 2004 Conference, June*, Vol. 3. 2004.
- [12] Brower, DV, Prescott, CN, Zhang, J, Howerter, C and Rafferty, D. "Real-time flow assurance monitoring with non-intrusive fiber optic technology." *Offshore Technology Conference*. 2005. Offshore Technology Conference.
- [13] Eaton, A., Safdarnejad, S.M., Hedengren, J.D., Moffat, K., Hubbell, C., Brower, D.V. and Brower, A.D. "Post-Installed Fiber Optic Pressure Sensors on Subsea Production Risers for Severe Slugging Control." *ASME 34th International Conference on Ocean, Offshore, and Arctic Engineering (OMAE)*. 42196. 2015. St. John's, Newfoundland, Canada.
- [14] Brower, D., Hedengren, J.D., Shishivan, R. Asgharzadeh and Brower, A. "Advanced Deepwater Monitoring System." *Ocean, Offshore & Arctic Engineering OMAE*. 10920. 2013. Nantes, France.
- [15] Brower, D., Hedengren, J.D., Loegering, C., Brower, A., Witherow, K. and Winter, K. "Fiber Optic Monitoring of Subsea Equipment." *Ocean, Offshore & Arctic Engineering OMAE*. 84143. 2012. Rio de Janeiro, Brazil.
- [16] Brower, David V, Brower, Alexis, Asgharzadeh Shishavan, Reza and Hedengren, John D. "A Post-Installed Subsea Monitoring System for Structural and Flow Assurance Evaluation." *Offshore Technology Conference*. OTC 25368. 2014. Houston, Texas.
- [17] Asgharzadeh Shishavan, Reza, Hedengren, John D., Brower, David V and Brower, Alexis. "New Advances in Post-Installed Subsea Monitoring Systems for Structural and Flow Assurance Evaluation." *ASME 33rd International Conference on Ocean, Offshore, and Arctic Engineering OMAE*. OMAE2014/24300. 2014. San Francisco, California.
- [18] Brower, D.V., Bentley, N.L., Hedengren, J.D., Kipp, R.M., Le, S.Q., Seaman, C., Tang, H.H. and Wilson, J.C. "Full-Scale Testing of a Friction-Based, Post-Installable, Fiber-Optic Strain Sensor for Subsea Monitoring Systems." *ASME 37th International Conference on Ocean, Offshore, and Arctic Engineering OMAE*. OMAE2018/77117. 2018. Madrid, Spain.
- [19] Liu, Xin, Jin, Baoquan, Bai, Qing, Wang, Yu, Wang, Dong and Wang, Yuncai. "Distributed fiber-optic sensors for vibration detection." *Sensors* Vol. 16 No. 8 (2016): p. 1164.
- [20] Brower, D.V., Hedengren, J.D., Seaman, C. and Wilson, J.C. "A Post-Installable Fiber-Optic Sensor System for Leak Detection using Acoustic and Vibration Monitoring." *ASME 38th International Conference on Ocean, Offshore, and Arctic Engineering OMAE*. OMAE2019/95558. 2019. Glasgow, Scotland, UK.
- [21] Prescott, CN, Zhang, J, Brower, DV et al. "An ambient pressure insulated LNG pipeline for subsea environments." *Offshore Technology Conference*. 2005. Offshore Technology Conference.